Published in final edited form as:

Environ Microbiol. 2017 October ; 19(10): 3982–3996. doi:10.1111/1462-2920.13798.

The ArfGAP protein MoGlo3 regulates the development and pathogenicity of *Magnaporthe oryzae*

Shengpei Zhang[1], **Xiu Liu**[1], **Lianwei Li**[1], **Rui Yu**[1], **Jialiang He**[1], **Haifeng Zhang**[1], **Xiaobo Zheng**[1], **Ping Wang**[2], and **Zhengguang Zhang**[1,*]

[1]Department of Plant Pathology, College of Plant Protection, Nanjing Agricultural University, and Key Laboratory of Integrated Management of Crop Diseases and Pests, Ministry of Education, Nanjing 210095, China

[2]Departments of Pediatrics, and Microbiology, Immunology, and Parasitology, Louisiana State University Health Sciences Center, New Orleans, Louisiana 70112, USA

Abstract

The ADP ribosylation factor (Arf) and the coat protein complex I (COPI) are both involved in vesicle transport. Together with GTPase-activating proteins (ArfGAPs) and guanine exchange factors (ArfGEFs) that regulate the activity of Arf, they govern vesicle formation, COPI trafficking, and the maintenance of the Golgi complex. In an ongoing effort to study the role of membrane trafficking in pathogenesis of the rice blast fungus *Magnaporthe oryzae*, we identified MoGlo3 as an ArfGAP protein that is homologous to Glo3p of the budding yeast *Saccharomyces cerevisiae*. As suspected, MoGlo3 partially complements the function of yeast Glo3p. Consistent with findings in *S. cerevisiae*, MoGlo3 is localized to the Golgi and that the localization is dependent on the conserved BoCCS domain. We found that MoGlo3 is highly expressed during conidiation and early infection stages, and is required for vegetative growth, conidial production, and sexual development. We further found that the Δ*Moglo3* mutant is defective in endocytosis, scavenging of the reactive oxygen species (ROS), and in the response to endoplasmic reticulum (ER) stress. The combined effects result in failed appressorium function and decreased pathogenicity. Moreover, we provided evidence showing that the domains including the GAP, BoCCS and GRM are all important for normal MoGlo3 functions. Our studies further illustrate the importance of normal membrane trafficking in the physiology and pathogenicity of the rice blast fungus.

Introduction

Owing to its economic and biological importance, *Magnaporthe oryzae* has been regarded as an excellent model for studying fungal pathogen–plant interactions (Howard and Valent, 1996; Ebbole, 2007). In studying molecular mechanisms of rice blast caused by *M. oryzae*, we previously discovered that soluble N-ethylmaleimide-sensitive factor attachment protein receptors (SNAREs) MoSec22, MoVam7, and MoSyn8 involved in membrane trafficking play important roles in conidiation, appressorium function, and pathogenesis (Song et al.,

*Corresponding author: Zhengguang Zhang, zhgzhang@njau.edu.cn, Tel: 86-25-84396972, Fax: 86-25-84396436.

2010; Dou et al., 2011; Qi et al., 2016). To further address functions of SNARE proteins, we identified an ADP ribosylation factor (Arf) small GTPase (ArfGAP) MoGlo3, whose homologs are thought to promote conformational changes of SNAREs that are essential for the trafficking of membrane-coated cargo between organelles (Pelham, 1999; Rein et al., 2002; Schindler and Spang, 2007).

In vesicle tracking of eukaryotic cells, coatomer protein I (COPI) vesicles are required for retrograde traffic from the Golgi to the ER (Letourneur et al., 1994) while coatomer protein II (COPII) vesicles are involved in transport from the endoplasmic reticulum (ER) to the Golgi (Barlowe et al., 1994). The small G protein ADP-ribosylation factor (Arf1) plays a key role in the generation of COPI (D'Souza-Schorey and Chavrier, 2006; Yorimitsu et al., 2014). The function of Arf is regulated by guanine nucleotide exchange factors (ArfGEFs) and GTPase-activating proteins (ArfGAPs) (Tanigawa et al., 1993; Lewis et al., 2004; D'Souza-Schorey and Chavrier, 2006; Gillingham and Munro, 2007; Yorimitsu et al., 2014).

Two major classes of ArfGAP, ArfGAP1 and AZAP, have been identified. ArfGAP1 has an ArfGAP domain at the N-terminus, and the AZAP class has an ArfGAP domain sandwiched between the PH and ankyrin (ANK) repeat domains (Inoue and Randazzo, 2007). In addition, the ArfGAP group is subdivided into distinct subclasses: ArfGAP1 and ArfGAP2/3 (Inoue and Randazzo, 2007; Schindler et al., 2009). ArfGAP2/3 is also named as Glo3-type ArfGAP that is highly conserved among various species. The single yeast Glo3 protein is required for COPI coat assembly and vesicle formation (Lewis et al., 2004; Kartberg et al., 2010). There are three Glo3-type ArfGAPs (AGD8, AGD9, AGD10) found in *Arabidopsis* that are responsible for Golgi maintenance and plant growth (Min et al., 2013). Two homologues of Glo3 in *Rattus norvegicus* (ARFGAP2, ARFGAP3) also regulates the COPI trafficking (Weimer et al., 2008). Despite the importance, little information is available regarding functions of such proteins in filamentous fungi including *M. oryzae*.

To further assess the roles of SNARE protein mediated vesicle trafficking in pathogenesis of the rice blast, we identified MGG_01472 as a homolog of Glo3-type ArfGAP in *M. oryzae* and characterized its function. We provided evidence demonstrating that MoGlo3 is also required for normal cellular transport and for normal growth, differentiation, and pathogenicity.

Results

Identification of a Glo3-type ArfGAP from *M. oryzae* and its expression

Since previous studies suggest that Glo3-type ArfGAPs are conserved from yeasts to animals and plants, we searched available genomes of *M. oryzae* (http://fungidb.org/fungidb/) and identified MGG_01472 as a homolog of *S. cerevisiae* Glo3p that we named MoGlo3. MoGlo3 was predicted to encode 490 amino acids and phylogenetic analysis confirmed sequence conservation among similar proteins. MoGlo3 shared high amino acid sequence homology with that of apple tree pathogen *Valsa mali* (80 % identify and 87 % similarity) and lesser homology with yeast Glo3p (33 % identify and 48 % similarity) (Fig. 1A). A further amino acid sequence alignment showed that Glo3-type ArfGAPs contains a conserved GAP domain in the N-terminal region, which is of ~140 amino acid residues and

include an invariant of C-X_2-CX_{16-17}-C-X_2-C-X_4-R motif (Gillingham and Munro, 2007), redundant KK motifs in the center (Kliouchnikov et al., 2009) and repeated ISSxxxFG sequences proximal to the C-terminus (Yahara et al., 2006) (Fig. S1).

To test for any functional conservation, we expressed MoGlo3 in a Δ*Scglo3* mutant using the yeast expression vector pYES2. We found that MoGlo3 could rescue the function of ScGlo3p, albeit partially. This evidence suggests that MoGlo3 is likely a Glo3-type of ArfGAP (Fig. 1B).

To further characterize the functions of *MoGLO3*, we performed a quantitative real-time reverse transcription polymerase chain reaction (qRT-PCR) analysis at different development stages of the fungus. The relative quantification of transcript levels normalized to actin (MGG_03982) showed that *MoGLO3* transcript abundance at the conidial stage, 8 h post-inoculation (hpi) and 24 hpi, was 2.6-, 4.2-, and 6.1-fold, respectively, relative to that of the hyphal stage (Fig. S2). The evidence implies the importance of MoGlo3 during the conidial and early infectious stages.

MoGlo3 plays a role in endocytosis

To examine the function of MoGlo3, we performed targeted *MoGLO3* gene disruption by replacing the coding region with a hygromycin-resistance cassette (*HPH*) (Fig. S3A). The Δ*Moglo3* mutant was confirmed by Southern blot analysis (Fig. S3B) and the mutant was also complemented with the wild-type *MoGLO3* gene that restored all defects.

Previous study showed that deletion of *GLO3* affect the endocytic recycling of cell-surface proteins (Kawada et al., 2015). To determine whether MoGlo3 plays the similar role, we stained the hypha of wild-type Guy11, Δ*Moglo3* mutant, and complemented strain Δ*Moglo3/MoGLO3* with the lipophilic styryl dye FM4-64, which is an endocytic tracer (Fischer-Parton et al., 2000; Gilbert et al., 2006). FM4-64 was internalized in the hypha of the wild-type and complemented strain after 1 min exposure, but few hypha of the Δ*Moglo3* mutant were internally stained. After 3 min, the dye remained on the plasma membrane, and up to 5 min, staining was comparable to that of Guy11 and the complemented strain (Fig. 2A). The assessment of fluorescent density (Fig. 2B) was consistent in indicating that MoGlo3 plays a role in early endocytosis.

MoGlo3 plays a critical role in vegetative growth

To assess the growth, the Guy11, Δ*Moglo3* and Δ*Moglo3/MoGLO3* strain were cultured on complete medium (CM), oatmeal agar medium (OM), minimal medium (MM), and straw decoction and corn medium (SDC). After growth at 28°C for 7 days, the Δ*Moglo3* mutant showed significantly reduced radial growth on all four media (Fig. 3A and B). Similar results were observed following incubation in liquid CM for 48 h (Fig. 3C), suggesting that MoGlo3 is required for normal vegetative growth.

MoGlo3 is involved in asexual and sexual development

Conidia act as the primary infectious particles and is important in the disease cycle of rice blast (Lee et al., 2006; Zhang et al., 2016). To examine the function of MoGlo3 in

conidiation, Guy11, Δ*Moglo3* and Δ*Moglo3/MoGLO3* were observed following the induction of conidiation on glass slides for 16 h. The Δ*Moglo3* mutant produced fewer conidiophores and conidia than the wild-type and complemented strain (Fig. 4A, upper panel). To validate this result, numbers of conidia produced on SDC medium for 10 days were determined. Consistently, Δ*Moglo3* produced significant fewer conidia than the wild-type and complemented strain (Fig. 4A, lower panel).

A series of genes related to spore production have been identified in plant pathogens, including *CON2*, *STUA*, *HOX2*, *COS1*, *COM1* and *CON7* (Shi and Leung, 1995; Kim et al., 2009; Nishimura et al., 2009; Zhou et al., 2009; Yang et al., 2010). Therefore, we examined the expression of these genes in Guy11 and Δ*Moglo3* by qRT-PCR. The transcript level of *MoCOS1* was reduced about 5-fold in Δ*Moglo3* mutant and the transcripts of *MoSTUA*, *MoCOM1*, *MoCON7* were also reduced significantly in the Δ*Moglo3* mutant (Fig. 4B).

To investigate the role of MoGlo3 in sexual development, the wild-type, *ΔMoglo3* and complemented strain (*MAT1-2*) were crossed with the standard test strain TH3 (*MAT1-1*). Four weeks later, numerous perithecia were observed at the junctions of the wild-type and complemented strain with TH3, but not *ΔMoglo3* (Fig. 4C, upper panel). The same result was also found for ascus and ascospore production (Fig. 4C, lower panel). These results suggest that MoGlo3 plays an essential role in sexual development.

MoGlo3 is required for full virulence

As conidia production was severely impaired, we sprayed equal conidial suspensions (only 1×10^4 conidia/ml) of Guy11, Δ*Moglo3*, and Δ*Moglo3/MoGLO3* on the 2-week-old rice seedlings. After 7 days, the Δ*Moglo3* mutant produced a few pinhead-sized brown specks, in contrast to the numerous and typical lesions produced by the wild-type and complemented strain (Fig. 5A). The similar result was observed in the injected sheath assay (Fig. 5B). The pinhead-sized specks caused by Δ*Moglo3* mutant could not produce conidia under the illuminated induction condition (Fig. 5C). A similar decrease in pathogenicity was also obtained in a detached barley assay. The controls showed severe blast symptoms after 5 days, whereas the Δ*Moglo3* mutant produced few restricted lesions on leaves. Moreover, the assay using wounded leaves for infection showed a significantly reduced virulence by the Δ*Moglo3* mutant that produced minimal expanded lesions (Fig. 5D).

To explore the possible cause of pathogenicity defect, we observed the penetration and invasive hyphae growth of the Δ*Moglo3* mutant in rice sheath cells. At least 90% of appressorium penetration and 65% extended invasive hyphae at 24 hpi seen in the wild-type strain, 95% of the mutant appressoria failed to penetrate the cell wall (Fig. 5E). To further elaborate these observations, we extended for 48 hpi to quantify the penetration and infectious hyphal growth using four types of rice cell. In the wild-type and complemented strain, more than 75% of the penetration sites were Type 3 (30% and 33%) and Type 4 (49% and 45%), only less than 25% of the cells showed Type 1 (6% and 5%) and Type 2 (15% and 17%). In contrast, more than 90% of the Δ*Moglo3* hyphae were Type 1, Type 2 (4%) and Type 3 (3%) were less than 10%, and none of the hyphae showed Type 4 (Fig. 5F). Moreover, we also observed the invasive hyphal growth in barley leaves at 24 hpi from Type

1 to 4. In the wild-type and complemented strain, 48% and 46% of the penetration sites were Type 4, 10% and 8% were Type 1, respectively. However, in the Δ*Moglo3* mutant, 15% were Type 2 and 85% were Type 1 (Fig. 5G). These results, together with the wounding assay, suggest that the Δ*Moglo3* mutant has defects in appressorial penetration and infectious growth.

Since appressorium-mediated host penetration requires the maintenance of strong internal turgor pressure (deJong et al., 1997), we performed appressorial turgor measurement through a cytorrhysis assay (Howard et al., 1991). In 1 M glycerol, 33% of the appressoria exhibited cytorrhysis or plasmolysis in the Δ*Moglo3* mutant, compared with 15% and 14% of those in the wild-type and complemented strain, respectively. The total percentages of cytorrhysis plus plasmolysis (Wang et al., 2013b) were proportional to the external glycerol concentration, however the Δ*Moglo3* mutant retained a significantly higher rates than the wild-type and complemented strain (Fig. 5H), indicating a lower appressorial turgor in the Δ*Moglo3* mutant. These results suggest that Δ*Moglo3* mutant has decreased appressorial turgor that contributes to the defect in penetration and virulence.

MoGlo3 is involved in scavenging of reactive oxygen species (ROS)

In the interaction between rice blast fungus and rice, ROS generation acts as a defense mechanism to protect neighboring cells (Chi et al., 2009). Conversely, the rice blast fungus regulates the expression of redox homeostasis-related genes to detoxify host-driven ROS (Guo et al., 2011). Based on the restricted disease specks caused by the Δ*Moglo3* mutant being similar to resistant-type lesions on rice, we explored whether MoGlo3 is involved in ROS scavenging by measuring ROS production in rice cells using 3, 3′-Diaminobenzidine (DAB) staining at 30 hpi. Of rice cells infected with the Δ*Moglo3* mutant, 62% stained brown, compared to 12% and 14% of those infected with the wild-type and complemented strain, respectively (Fig. 6A and B). We assumed that the limitation of the invasive hyphae in infected cells and the decreased virulence of the Δ*Moglo3* mutant might be caused by a defect in host ROS scavenging. To test this hypothesis, we performed the excised leaf-sheath assay using diphenyleneiodonium (DPI) to inhibit the activity of NADPH oxidases, which are necessary generators of plant ROS (Cross and Jones, 1986; Chen et al., 2014a). Upon treatment with 0.5 μM DPI, some infectious hyphae of the Δ*Moglo3* mutant were seen spread into neighboring cells (Fig. 6C and D). These observations suggest that MoGlo3 is involved in scavenging ROS, and that the defect in the invasive growth of the Δ*Moglo3* mutant may be due in part to accumulation of ROS.

ROS is also known as a diffusible second messenger for defense signaling and defense gene induction (Nurnberger et al., 2004; Torres and Dangl, 2005). Therefore, to further investigate whether the plant defense genes were activated in infection by the Δ*Moglo3* mutant, we assayed the transcript levels of five defense-related genes that are involved in salicylic acid (SA) (*PR1a*, *Cht1*) or jasmonic acid (JA) (*Lox*, *PBZ1*, *AOS2*) pathways by qRT-PCR (Guo et al., 2010; Chen et al., 2014b). The transcript levels of all genes in rice infected with the Δ*Moglo3* mutant were much higher than with Guy11 at 24 hpi or 72 hpi, except the transcript level of *Lox* at 24 hpi, which showed no significant difference (Fig. 6E and F).

Taken together, we propose that the limited invasive hyphae of the Δ*Moglo3* mutant in rice cell might be due to accumulation of host-derived ROS that trigger plant defense responses.

MoGlo3 localizes to the Golgi apparatus

To further dissect the function of MoGlo3, we fused a green fluorescent protein (GFP) tag to the C-terminus of MoGlo3 and observed its subcellular localization. MoGlo3 was clearly visible as punctate green fluorescence in both conidia and hyphae. Since Glo3-type ArfGAPs are located in the Golgi in mammalian and *Arabidopsis* cells (Watson et al., 2004; Min et al., 2013), we assessed whether the punctate fluorescence represents Golgi structures. We fused the RFP tag to MoSft2, which is a homolog of the yeast Golgi marker Sft2p (Liu et al., 2005) and introduced it into the MoGlo3-GFP contained strain. We found that most green fluorescence was co-localized with MoSft2-RFP in conidia (Fig. 7A), and the spot green fluorescence in mid and tip regions of the vegetative hyphae was also co-localized with MoSft2-RFP (Fig. 7B). We observed additional conidia and found most MoGlo3 was merged with MoSft2 in the germ tube and appressorium (Fig. 7C). A similar co-localization pattern between MoGlo3 and MoSft2 was also observed in infectious hyphae at 24 hpi. Punctate fluorescence signal of GFP and RFP were overlapped during plant tissue invasion (Fig. 7D), supporting MoGlo3 is localized to the Golgi complex.

MoGlo3 participates in the response to ER and cell wall stress

The Golgi localization of MoGlo3 suggests that it too regulates COPI-related retrograde transport from the Golgi to the ER (Letourneur et al., 1994). A study in yeast also showed that depletion of both Glo3p and another ArfGAP, Gcs1p, caused ER abnormalities (Poon et al., 1999). We thus examined the sensitivity of the Δ*Moglo3* mutant to dithiothreitol (DTT) that induces ER-stress and found that the Δ*Moglo3* mutant is hypersensitive to DTT (Fig. 8A and B). In our previous study, we found that MoHac1 functions as a transcription factor in the conserved unfolded protein response (UPR) pathway to regulate the ER-stress, and loss of MoHac1 generates more negative effects on the expression of some UPR-regulated genes in response to ER-stress (Tang et al., 2015). Based on the result that the Δ*Moglo3* mutant was more sensitive to ER-stress, we explored whether the loss of MoGlo3 affects the UPR pathway through evaluating the transcript levels of a series of putative UPR-regulated genes as well as *MoHAC1*. The transcript levels of all detected genes, *MoSCJ1* (chaperone dnaJ 2), *MoKAR2* (ER protein chaperone BiP), *MoERV29* (ER-derived vesicles protein), *MoSEC61* (translocation of misfolded proteins out of ER), *MoDER1* (ER-associated degradation), *MoHAC1*, *MoSIL1* (a nucleotide exchange factor), were markedly increased in Guy11 upon treatment with DTT, but not to that levels in the Δ*Moglo3* mutant (Fig. 8C). Since the DTT-induced UPR pathway is related to the cell wall integrity (CWI) pathway (Tang et al., 2015; Yin et al., 2016), we tested the sensitivity of the Δ*Moglo3* mutant strain to three cell wall inhibitors, Calcofluor white (CFW), Congo red (CR), and sodium dodecyl sulfate (SDS). Consistently, all three exhibited significant inhibition to the Δ*Moglo3* mutant in comparison to the wild-type and complemented strain (Fig. S4).

The GAP, BoCCS and GRM domains are essential for the function of MoGlo3

The Glo3-type ArfGAPs are conserved GTPases containing the GAP, BoCCS and GRM domains (Fig. 9A) (Schindler et al., 2009). We investigated the contribution of each of these

domains for MoGlo3 functiuon in *M. oryzae*, and generated three domain-deleted strains (ΔGAP, ΔBoCCS, ΔGRM). We expected reduced pathogenicity in strains with domain specific deletion alleles. As expected, all of the domain-deleted strains showed decreased pathogenicity (Fig. 9B). However, there were still some differences found. The ΔGAP mutant strain showed very few lesions, similar to the Δ*Moglo3* mutant, whereas the ΔBoCCS and ΔGRM strains caused more lesions on sprayed/injected rice and caused expanded injuries on detached barley (Fig. 9B). Growth and conidiation assays also showed that the ΔGAP mutant strain had the same phenotype as the Δ*Moglo3* mutant and ΔBoCCS and ΔGRM strains showed moderate growth and conidiation rates between the Δ*Moglo3* mutant and Guy11 (Fig. 9C and D). These results indicate that the GAP, BoCCS and GRM domains share important but different roles in MoGlo3 function.

The BoCCS domain is required for the subcellular localization of MoGlo3

In addition to examining MoGlo3 domain specific function, we also examined their roles in subcellular localization by generating truncated MoGlo3 proteins with C-terminal GFP fusion and by evaluating their co-localizations with MoSft2-RFP. The GAP-deleted protein co-localized with MoSft2-RFP (Fig. 10), suggesting that the GAP domain of MoGlo3 is not essential for Golgi localization. Moreover, the GRM-deleted MoGlo3-GFP co-localized with the Golgi marker, but the BoCCS-deleted MoGlo3-GFP was distributed throughout the cytoplasm and did not co-localize with the marker protein. This finding is in agreement with studies in yeast that the BoCCS domain is important for the membrane–coatomer/cargo interaction (Schindler et al., 2009).

Discussion

The regulation of protein and membrane cargo transport among eukaryotic organelles supports the integrity and function of these compartments (Lewis et al., 2004). ArfGAP small GTPases function in generation and traffic of COPI, one of three types of coated vesicles regulating retrograde transport from the Golgi to the ER, and the highly conserved Glo3-type ArfGAPs involves in COPI coat assembly, vesicle formation and trafficking, and Golgi maintenance (Lewis et al., 2004; Weimer et al., 2008; Kartberg et al., 2010; Min et al., 2013). In this study, we identified one Glo3-type ArfGAP MoGlo3 in *M. oryzae*. We found that MoGlo3 not only has a conserved GAP domain in the N-terminal area, redundant KK motifs (BoCCS) in the central region, and repeated ISSxxxFG (GRM) sequences proximal to the C-terminus, but also can partially complement the growth defect of the Δ*Scglo3* mutant. Our findings suggest that MoGlo3 shares both structural and functional similarity to *S. cerevisiae* Glo3p.

Targeted gene deletion of *MoGLO3* revealed that MoGlo3 is involved in growth, which is consistent with previous studies in yeast and *Arabidopsis* (Poon et al., 1999; Brandizzi and Barlowe, 2013). The dramatically decreased conidiation in the Δ*Moglo3* mutant is consistent with the upregulated expression of *MoGLO3* at the conidial stage suggesting that MoGlo3 is critical for conidiogenesis. This reasoning is further supported by findings that the expression of some conidiation-related genes were reduced in the *ΔMoglo3* mutant. The 5-fold reduction of transcript level of *MoCOS1* which is a determinant of conidiophore (Zhou

et al., 2009) in the Δ*Moglo3* mutant suggests the down-regulation of *MoCOS1* causes the fewer conidiophores in the Δ*Moglo3* mutant. The transcript levels of *MoSTUA*, *MoCOM1*, and *MoCON7* were also significantly reduced in the *ΔMoglo3* mutant. Whereas the previous studies found that loss of *MoSTUA* or *MoCON7* causes dramatically decreased conidiation (Shi and Leung, 1995; Nishimura et al., 2009), and the *MoCOM1*-deleted mutant shows defects in conidium morphology (Yang et al., 2010). Interestingly, despite that MoCon2 and MoHox2 are also involved in the conidial development (Shi et al., 1998; Kim et al., 2009), their transcript levels were not significantly affected. Thus, the function of MoGlo3 in conidial development might include differential regulation of transcription for certain conidiation-related genes.

Previous studies found that deletion or RNA interference of *GLO3* caused abnormal Golgi compartmentation and endocytosis (Watson et al., 2004; Min et al., 2013; Kawada et al., 2015). In this study, we localized MoGlo3 to Golgi at different developmental stages, including hyphae, conidia, germ tube, appressorium and infectious hyphae, suggesting that Golgi localization is required for the function of MoGlo3. We also showed that MoGlo3 is required for normal endocytosis. Endocytosis is the process by which cells transfer extracellular material and plasma membrane proteins to internal compartments via intracellular trafficking (Goode et al., 2015). The endocytic defects of Δ*Moglo3* mutant indicate an imbalanced vesicle trafficking and abnormal collection of extracellular material, suggesting that the defect in absorption of materials results in growth defect of the mutant. A study in *Ustilago maydis* found that endocytosis is required for the initial steps of pathogenic development and spore formation (Fuchs et al., 2006). Our previous studies also showed that several proteins involved in endocytosis, including MoDnm1, MoSyn8, and MoArk1, also regulate conidiogenesis and pathogenesis (Wang et al., 2013a; Qi et al., 2016; Zhong et al., 2016). How exactly MoGlo3-mediated endocytosis affects conidiogenesis and pathogenesis remains unclear and further studies are necessary.

Studies in yeast showed that Glo3p is required for COPI-related retrograde transport from the Golgi to the ER and depletion of both Glo3p and Gcs1p resulted in ER abnormalities (Letourneur et al., 1994; Poon et al., 1999). By using DTT as an ER stress inducer, we demonstrated that MoGlo3 has a role in the ER stress response. In addition, we showed that MoGlo3 has a role in the UPR pathway mediated by MoHac1 and MoMck1 (Tang et al., 2015; Yin et al., 2016). Since ER stress is hypothesized to occur during infection and invasive hyphae growth and that the fully functional UPR is required for penetration and invasive hyphae growth (Tang et al., 2015), the perturbed UPR pathway under ER stress in the Δ*Moglo3* mutant might foretell a defect in pathogenicity.

We reasoned that the significantly decreased virulence in the Δ*Moglo3* mutant was due to two direct underlying mechanisms. First, the penetration rate of the mutant was markedly decreased, likely due to reduced appressorium internal turgor pressure. The pathogenicity of the Δ*Moglo3* mutant was partially restored when conidia were incubated on wounded barley. Secondly, the ROS-scavenging ability of the Δ*Moglo3* mutant was also reduced. In plants, ROS acts as one of the first responses to fungal invasion and ROS is known as a second messenger for defense signaling and defense gene induction (Mellersh et al., 2002; Nurnberger et al., 2004; Torres and Dangl, 2005). Plant pathogens detoxify host-driven ROS

to suppress ROS-mediated plant immunity (Molina and Kahmann, 2007; Chi et al., 2009), promoting expansion of invasive hyphae in plant cells.

Plants have salicylic acid (SA) signaling pathway and jasmonic acid (JA) signaling pathway, which defend pathogen invasion (Dong et al., 2015). Because of the defect in ROS scavenging, the transcript level of five defense-related genes (*PR1a*, *Cht1*, *PBZ1*, *AOS2*, *Lox*), which are involved in SA and JA pathway, were all upregulated (except for *Lox* at 24 hpi) in the Δ*Moglo3* mutant. This prevents the Δ*Moglo3* mutant from inhibiting ROS-mediated rice immunity and thus exhibited a defect in virulence. Consistently with this reasoning, the presence of DPI that inhibits ROS partially restored virulence when conidia were used to infect detached rice sheaths.

MoGlo3 contains the GAP, BoCCS and GRM domains that are also present in yeast Glo3p (Schindler et al., 2009). The GAP domain may be the most important domain, as the GAP-specific mutant strain exhibited similar defects as the Δ*Moglo3* mutant. This is because the GAP domain is required for GTP hydrolysis (Cukierman et al., 1995). Studies in other organisms found that the center region of ArfGAP3 interacts efficiently with a coatomer in *Homo sapiens* (Kliouchnikov et al., 2009), and that the repeated ISSxxxFG sequence motif regulates the function of yeast Glo3p (Yahara et al., 2006). However, another study of yeast Glo3p suggested that the GAP and BoCCS domains are sufficient for all essential functions and that GRM is dispensable for growth (Schindler et al., 2009). Here, our results suggest that GRM, like GAP and BoCCS, is also required for full function. Further, deletion of the GAP or GRM domain did not affect MoGlo3 localization to the Golgi and these domain-deleted proteins did not fully restore the Δ*Moglo3* mutant phenotype when reintroduced. Deletion of the BoCCS domain resulted in failed Golgi localization and this domain-deleted protein also could not fully complement the Δ*Moglo3* mutant phenotype when reintroduced. All these findings indicate that all three domains are important for the normal function of MoGlo3.

In summary, we identified and characterized a Glo3-type ArfGAP, MoGlo3, in *M. oryzae*. Our findings showed that MoGlo3 plays multifunctional roles in the growth and development of *M. oryzae*. The *ΔMoglo3* mutant is pleiotrophic in defects ranging from intracellular trafficking to growth, conidiation, appressorium turgor, ROS scavenging, ER stress response, and pathogenicity. Our studies provide new insight for the role of cellular transport in growth and development of pathogenic fungi that also highlight the importance of exploring such a new mean controlling fungal pathogenicity.

Materials and methods

Phylogenetic tree construction and sequence alignment

The Glo3-Type ArfGAP proteins of several organisms were acquired from NCBI database (https://www.ncbi.nlm.nih.gov/). Amino acid sequence alignment were made using the CLUSTAL_W programs and the calculated phylogenetic tree was constructed by MEGA 5.05 programs.

Complementation of the *Saccharomyces cerevisiae* Δ*Scglo3* mutant

The full length cDNA of *MoGLO3* was amplified using primers (Table S1), which is digested with XbaI and SacI, then cloned into the yeast expression vector pYES2 plasmid (Invitrogen). After verified by sequencing and selecting on SD medium lacking uracil, the *MoGLO3*-pYES2 vector was transformed into yeast Δ*Scglo3* mutant (BY4741, Δ*YRE122C*). Yeast strains were cultured on YPD medium and diluted to an OD600 of 0.1, after that 5 μl of 10-fold serial dilutions were grown on SD-Met-Leu-His-Ura (galactose) plates at 30°C for 4 days and then photographed.

Quantitative RT-PCR and analysis of gene expression

Total RNA of different *M. oryzae* developmental stages were extracted and reverse transcribed into first-strand cDNA with the Reverse transcription Kit (Vazyme). Relative quantification of transcriptional level was normalized to Actin (MGG_03982). To evaluate the transcriptional level of conidiation-related genes and UPR-related genes, total RNA of Guy11 and Δ*Moglo3* mutant with or without DTT treatment were performed as the method above and analyzed by Duncan analysis. For the transcript levels of defense-related genes, total RNA of rice infected with Δ*Moglo3* mutant and wide-type at 0, 24 and 72 h were extracted.

Strains and culture conditions

M. oryzae Guy11 was used as the wild-type strain in this study, and unless the mentioned medium, all of the strains were cultured on CM plate at 28°C in darkness. For preparing the DNA, RNA and protein extractions, fungal mycelia were harvested after incubated in liquid CM for 2 days. For the stress inducers, the concentrations were 2.5 mM to DTT, 200 μg/ml to CFW, 200 μg/ml to Congo red, 0.005% to SDS.

Gene deletion and complementation

The *MoGLO3* was substituent with hygromycin resistance cassette (*HPH*) by the standard one-step gene replacement strategy. Approximately 1.0-kb DNA fragments franking the targeted *MoGLO3* were amplified with the primer pairs (Table S1). The upstream and downstream sequences were digested by XhoI, EcoRI and SpeI, SacII respectively. Then we cloned them into a pCX62 vector contained *HPH* (Fig. S3A). The constructed plasmid was transformed into wide-type Guy11, putative Δ*Moglo3* mutant was screened by PCR and further confirmed by Southern blotting analysis (Fig. S3B). As for the complement assay, the full-length of *MoGLO3* (except stop codon) and approximately 1.5-kb native promoter area of it were amplified and cloned into pYF11 vector (bleomycin resistance), then transformed it to Δ*Moglo3* mutant for complementation, transformants were selected as described previously (Liu et al., 2016).

Endocytosis assays

To examine endocytosis, the strains were cultured in liquid CM for 24 h before FM4-64 (Molecular Probes Inc., Eugene, OR, USA) staining. Then the samples were washed by ddH_2O four times and photographs were taken (Zeiss LSM710, 63x oil). The relative

integrated density of the fluorescent photographs was analyzed by IMAGE-PRO PLUS (Media Cybernetics Inc., Shanghai, China).

Conidiation and sexual reproduction

Conidiation were acquired as the method in the reference (Wang et al., 2013a), then counted and analyzed by Duncan analysis. Sexual reproduction assay was started with Guy11 and related strains (*MAT1-2*) culturing together with standard TH3 (*MAT1-1*) strain on OM plates 4 days, then incubated in continuous white light at 20°C 4 weeks (Zhang et al., 2011).

Pathogenicity assays

For plant pathogenicity assays, equal concentration (5×10^4 or 1×10^4 conidia/ml) conidial suspensions with 0.2% (w/v) gelatin were incubated to rice (*Oryza sativa* cv. CO39) or detached barleys, which were first kept in a chamber at 25°C, 90% humidity and in darkness then followed by a light/dark cycle (Wang et al., 2016). For the injection assay, 1.5 ml of conidial suspensions (5×10^4 conidia/ml) were injected into more than 20 leaf sheaths of rice seedlings with needles. Lesions around the inoculation sites were observed when the injection-wounded leaves unfolded after 7 dpi, as described previously (Xu and Hamer, 1996; Qi et al., 2016). For microscopic observation of the invasive hypha in host cells, conidial suspensions were inoculated to detached sheaths or barleys in darkness. After 24 or 48 hpi, the inner host cells were observed and classified.

Host-derived ROS observation

ROS was detected by staining with DAB (Sigma-Aldrich) following the conidia incubating rice sheaths 30 h, and 0.5 μM DPI was mixed with the conidial suspensions to inhibit the stress caused by ROS. The detailed methods were as described (Chen et al., 2014a; Wang et al., 2016).

Localized observation

To observe the subcellular localization of MoGlo3, we fused MoGlo3 or truncated MoGlo3 with a GFP tag and the Golgi marker MoSft2 with a RFP tag. Green and red fluorescence of conidia and different developmental stages of conidia were examined under confocal fluorescence microscope (Leica TCS SP8, 100x oil). Vegetative and infectious hypha were also observed by the two fluorescence (Zeiss LSM710, 63x oil).

Supplementary Material

Refer to Web version on PubMed Central for supplementary material.

Acknowledgments

This research was supported by the key program of Natural Science Foundation of China (Grant No: 31530063, ZZ), National Science Foundation for Distinguished Young Scholars of China (Grant No.31325022 to ZZ), Natural Science Foundation of China (Grant No: 31470248, XZ). The Wang laboratory research was supported by NIH grants AI121460 and AI121451 (USA).

References

Barlowe C, Orci L, Yeung T, Hosobuchi M, Hamamoto S, Salama N, et al. COPII: a membrane coat formed by Sec proteins that drive vesicle budding from the endoplasmic reticulum. Cell. 1994; 77:895–907. [PubMed: 8004676]

Brandizzi F, Barlowe C. Organization of the ER-Golgi interface for membrane traffic control. Nat Rev Mol Cell Biol. 2013; 14:382–392. [PubMed: 23698585]

Chen XL, Shi T, Yang J, Shi W, Gao X, Chen D, et al. N-glycosylation of effector proteins by an alpha-1,3-mannosyltransferase is required for the rice blast fungus to evade host innate immunity. Plant Cell. 2014a; 26:1360–1376. [PubMed: 24642938]

Chen Y, Zhai S, Zhang H, Zuo R, Wang J, Guo M, et al. Shared and distinct functions of two Gti1/Pac2 family proteins in growth, morphogenesis and pathogenicity of Magnaporthe oryzae. Environ Microbiol. 2014b; 16:788–801. [PubMed: 23895552]

Chi MH, Park SY, Kim S, Lee YH. A novel pathogenicity gene is required in the rice blast fungus to suppress the basal defenses of the host. PLoS Pathog. 2009; 5

Cross AR, Jones OTG. The effect of the inhibitor diphenylene iodonium on the superoxide-generating system of neutrophils - specific labeling of a component polypeptide of the oxidase. Biochem J. 1986; 237:111–116. [PubMed: 3800872]

Cukierman E, Huber I, Rotman M, Cassel D. The Arf1 GTPase-activating protein - zinc-finger motif and Golgi-complex localization. Science. 1995; 270:1999–2002. [PubMed: 8533093]

D'Souza-Schorey C, Chavrier P. ARF proteins: roles in membrane traffic and beyond. Nat Rev Mol Cell Biol. 2006; 7:347–358. [PubMed: 16633337]

deJong JC, MCCormack BJ, Smirnoff N, Talbot NJ. Glycerol generates turgor in rice blast. Nature. 1997; 389:244–245.

Dong Y, Li Y, Zhao M, Jing M, Liu X, Liu M, et al. Global genome and transcriptome analyses of Magnaporthe oryzae epidemic isolate 98-06 uncover novel effectors and pathogenicity-related genes, revealing gene gain and lose dynamics in genome evolution. Plos Pathog. 2015; 11:e1004801. [PubMed: 25837042]

Dou X, Wang Q, Qi Z, Song W, Wang W, Guo M, et al. MoVam7, a conserved SNARE involved in vacuole assembly, is required for growth, endocytosis, ROS accumulation, and pathogenesis of Magnaporthe oryzae. PLoS One. 2011; 6:e16439. [PubMed: 21283626]

Ebbole DJ. Magnaporthe as a model for understanding host-pathogen interactions. Annu Rev Phytopathol. 2007; 45:437–456. [PubMed: 17489691]

Fischer-Parton S, Parton RM, Hickey PC, Dijksterhuis J, Atkinson HA, Read ND. Confocal microscopy of FM4-64 as a tool for analysing endocytosis and vesicle trafficking in living fungal hyphae. J Microsc. 2000; 198:246–259. [PubMed: 10849201]

Fuchs U, Hause G, Schuchardt I, Steinberg G. Endocytosis is essential for pathogenic development in the corn smut fungus Ustilago maydis. Plant Cell. 2006; 18:2066–2081. [PubMed: 16798890]

Gilbert MJ, Thornton CR, Wakley GE, Talbot NJ. A P-type ATPase required for rice blast disease and induction of host resistance. Nature. 2006; 440:535–539. [PubMed: 16554820]

Gillingham AK, Munro S. The small G proteins of the Arf family and their regulators. Annu Rev Cell Dev Biol. 2007; 23:579–611. [PubMed: 17506703]

Goode BL, Eskin JA, Wendland B. Actin and endocytosis in budding yeast. Genetics. 2015; 199:315–358. [PubMed: 25657349]

Guo M, Chen Y, Du Y, Dong YH, Guo W, Zhai S, et al. The bZIP transcription factor MoAP1 mediates the oxidative stress response and is critical for pathogenicity of the rice blast fungus Magnaporthe oryzae. PLoS Pathog. 2011; 7

Guo M, Guo W, Chen Y, Dong SM, Zhang X, Zhang HF, et al. The basic leucine zipper transcription factor Moatf1 mediates oxidative stress responses and is necessary for full virulence of the rice blast fungus Magnaporthe oryzae. Mol Plant Microbe Interact. 2010; 23:1053–1068. [PubMed: 20615116]

Howard RJ, Valent B. Breaking and entering: host penetration by the fungal rice blast pathogen Magnaporthe grisea. Annu Rev Microbiol. 1996; 50:491–512. [PubMed: 8905089]

Howard RJ, Ferrari MA, Roach DH, Money NP. Penetration of hard substrates by a fungus employing enormous turgor pressures. Proc Natl Acad Sci U S A. 1991; 88:11281–11284. [PubMed: 1837147]

Inoue H, Randazzo PA. Arf GAPs and their interacting proteins. Traffic. 2007; 8:1465–1475. [PubMed: 17666108]

Kartberg F, Asp L, Dejgaard SY, Smedh M, Fernandez-Rodriguez J, Nilsson T, Presley JF. ARFGAP2 and ARFGAP3 are essential for COPI coat assembly on the Golgi membrane of living cells. J Biol Chem. 2010; 285:36709–36720. [PubMed: 20858901]

Kawada D, Kobayashi H, Tomita T, Nakata E, Nagano M, Siekhaus DE, et al. The yeast Arf-GAP Glo3p is required for the endocytic recycling of cell surface proteins. Biochim Biophys Acta. 2015; 1853:144–156. [PubMed: 25409928]

Kim S, Park SY, Kim KS, Rho HS, Chi MH, Choi J, et al. Homeobox transcription factors are required for conidiation and appressorium development in the rice blast fungus Magnaporthe oryzae. PLoS Genet. 2009; 5

Kliouchnikov L, Bigay J, Mesmin B, Parnis A, Rawet M, Goldfeder N, et al. Discrete determinants in ArfGAP2/3 conferring Golgi localization and regulation by the COPI coat. Mol Biol Cell. 2009; 20:859–869. [PubMed: 19109418]

Lee K, Singh P, Chung WC, Ash J, Kim TS, Hang L, Park S. Light regulation of asexual development in the rice blast fungus, Magnaporthe oryzae. Fungal Genet Biol. 2006; 43:694–706. [PubMed: 16765070]

Letourneur F, Gaynor EC, Hennecke S, Demolliere C, Duden R, Emr SD, et al. Coatomer is essential for retrieval of dilysine-tagged proteins to the endoplasmic-reticulum. Cell. 1994; 79:1199–1207. [PubMed: 8001155]

Lewis SM, Poon PP, Singer RA, Johnston GC, Spang A. The ArfGAP Glo3 is required for the generation of COPI vesicles. Mol Biol Cell. 2004; 15:4064–4072. [PubMed: 15254269]

Liu XY, Qian B, Gao CY, Huang SH, Cai YC, Zhang HF, et al. The putative protein phosphatase MoYvh1 functions upstream of MoPdeH to regulate the development and pathogenicity in Magnaporthe oryzae. Mol Plant Microbe Interact. 2016; 29:496–507. [PubMed: 27110741]

Liu YW, Huang CF, Huang KB, Lee FJ. Role for Gcs1p in regulation of Arl1p at trans-Golgi compartments. Mol Biol Cell. 2005; 16:4024–4033. [PubMed: 15975906]

Mellersh DG, Foulds IV, Higgins VJ, Heath MC. H2O2 plays different roles in determining penetration failure in three diverse plant-fungal interactions. Plant J. 2002; 29:257–268. [PubMed: 11844104]

Min MK, Jang M, Lee M, Lee J, Song K, Lee Y, et al. Recruitment of Arf1-GDP to Golgi by Glo3p-type ArfGAPs is crucial for Golgi maintenance and plant growth. Plant Physiol. 2013; 161:676–691. [PubMed: 23266962]

Molina L, Kahmann R. An Ustilago maydis gene involved in H2O2 detoxification is required for virulence. Plant Cell. 2007; 19:2293–2309. [PubMed: 17616735]

Nishimura M, Fukada J, Moriwaki A, Fujikawa T, Ohashi M, Hibi T, Hayashi N. Mstu1, an APSES transcription factor, is required for appressorium-mediated infection in Magnaporthe grisea. Biosci Biotechnol Biochem. 2009; 73:1779–1786. [PubMed: 19661696]

Nurnberger T, Brunner F, Kemmerling B, Piater L. Innate immunity in plants and animals: striking similarities and obvious differences. Immunol Rev. 2004; 198:249–266. [PubMed: 15199967]

Pelham HRB. SNAREs and the secretory pathway - lessons from yeast. Exp Cell Res. 1999; 247:1–8. [PubMed: 10047442]

Poon PP, Cassel D, Spang A, Rotman M, Pick E, Singer RA, Johnston GC. Retrograde transport from the yeast Golgi is mediated by two ARF GAP proteins with overlapping function. EMBO J. 1999; 18:555–564. [PubMed: 9927415]

Qi Z, Liu M, Dong Y, Zhu Q, Li L, Li B, et al. The syntaxin protein (MoSyn8) mediates intracellular trafficking to regulate conidiogenesis and pathogenicity of rice blast fungus. New Phytol. 2016; 209:1655–1667. [PubMed: 26522477]

Rein U, Andag U, Duden R, Schmitt HD, Spang A. ARF-GAP-mediated interaction between the ER-Golgi v-SNAREs and the COPI coat. J Cell Biol. 2002; 157:395–404. [PubMed: 11970962]

Schindler C, Spang A. Interaction of SNAREs with ArfGAPs precedes recruitment of Sec18p/NSF. Mol Biol Cell. 2007; 18:2852–2863. [PubMed: 17522384]

Schindler C, Rodriguez F, Poon PP, Singer RA, Johnston GC, Spang A. The GAP domain and the SNARE, coatomer and cargo interaction region of the ArfGAP2/3 Glo3 are sufficient for Glo3 function. Traffic. 2009; 10:1362–1375. [PubMed: 19602196]

Shi ZX, Leung H. Genetic analysis of sporulation in Magnaporthe grisea by chemical and insertional mutagenesis. Mol Plant Microbe Interact. 1995; 8:949–959.

Shi ZX, Christian D, Leung H. Interactions between spore morphogenetic mutations affect cell types, sporulation, and pathogenesis in Magnaporthe grisea. Mol Plant Microbe Interact. 1998; 11:199–207. [PubMed: 9487695]

Song W, Dou X, Qi Z, Wang Q, Zhang X, Zhang H, et al. R-SNARE homolog MoSec22 is required for conidiogenesis, cell wall integrity, and pathogenesis of Magnaporthe oryzae. PLoS One. 2010; 5:e13193. [PubMed: 20949084]

Tang W, Ru Y, Hong L, Zhu Q, Zuo R, Guo X, et al. System-wide characterization of bZIP transcription factor proteins involved in infection-related morphogenesis of Magnaporthe oryzae. Environ Microbiol. 2015; 17:1377–1396. [PubMed: 25186614]

Tanigawa G, Orci L, Amherdt M, Ravazzola M, Helms JB, Rothman JE. Hydrolysis of bound GTP by ARF protein triggers uncoating of Golgi-derived COP-coated vesicles. J Cell Biol. 1993; 123:1365–1371. [PubMed: 8253837]

Torres MA, Dangl JL. Functions of the respiratory burst oxidase in biotic interactions, abiotic stress and development. Curr Opin Plant Biol. 2005; 8:397–403. [PubMed: 15939662]

Wang J, Du Y, Zhang H, Zhou C, Qi Z, Zheng X, et al. The actin-regulating kinase homologue MoArk1 plays a pleiotropic function in Magnaporthe oryzae. Mol Plant Pathol. 2013a; 14:470–482. [PubMed: 23384308]

Wang J, Yin Z, Tang W, Cai X, Gao C, Zhang H, et al. The thioredoxin MoTrx2 protein mediates ROS balance and controls pathogenicity as a target of the transcription factor MoAP1 in Magnaporthe oryzae. Mol Plant Pathol. 2016

Wang J, Zhang Z, Wang Y, Li L, Chai R, Mao X, et al. PTS1 peroxisomal import pathway plays shared and distinct roles to PTS2 pathway in development and pathogenicity of Magnaporthe oryzae. PLoS One. 2013b; 8:e55554. [PubMed: 23405169]

Watson PJ, Frigerio G, Collins BM, Duden R, Owen DJ. gamma-COP appendage domain - Structure and function. Traffic. 2004; 5:79–88. [PubMed: 14690497]

Weimer C, Beck R, Eckert P, Reckmann I, Moelleken J, Brugger B, Wieland F. Differential roles of ArfGAP1, ArfGAP2, and ArfGAP3 in COPI trafficking. J Cell Biol. 2008; 183:725–735. [PubMed: 19015319]

Xu JR, Hamer JE. MAP kinase and cAMP signaling regulate infection structure formation and pathogenic growth in the rice blast fungus Magnaporthe grisea. Genes Dev. 1996; 10:2696–2706. [PubMed: 8946911]

Yahara N, Sato K, Nakano A. The Arf1p GTPase-activating protein Glo3p executes its regulatory function through a conserved repeat motif at its C-terminus. J Cell Sci. 2006; 119:2604–2612. [PubMed: 16735437]

Yang J, Zhao XY, Sun J, Kang ZS, Ding SL, Xu JR, Peng YL. A novel protein Com1 is required for normal conidium morphology and full virulence in Magnaporthe oryzae. Mol Plant Microbe Interact. 2010; 23:112–123. [PubMed: 19958144]

Yin Z, Tang W, Wang J, Liu X, Yang L, Gao C, et al. Phosphodiesterase MoPdeH targets MoMck1 of the conserved mitogen-activated protein (MAP) kinase signalling pathway to regulate cell wall integrity in rice blast fungus Magnaporthe oryzae. Mol Plant Pathol. 2016; 17:654–668. [PubMed: 27193947]

Yorimitsu T, Sato K, Takeuchi M. Molecular mechanisms of Sar/Arf GTPases in vesicular trafficking in yeast and plants. Front Plant Sci. 2014; 5:411. [PubMed: 25191334]

Zhang H, Tang W, Liu K, Huang Q, Zhang X, Yan X, et al. Eight RGS and RGS-like proteins orchestrate growth, differentiation, and pathogenicity of Magnaporthe oryzae. PLoS Pathog. 2011; 7:e1002450. [PubMed: 22241981]

Zhang HF, Zheng XB, Zhang ZG. The Magnaporthe grisea species complex and plant pathogenesis. Mol Plant Pathol. 2016; 17:796–804. [PubMed: 26575082]

Zhong K, Li X, Le X, Kong X, Zhang H, Zheng X, et al. MoDnm1 dynamin mediating peroxisomal and mitochondrial fission in complex with MoFis1 and MoMdv1 is important for development of functional appressorium in Magnaporthe oryzae. PLoS Pathog. 2016; 12:e1005823. [PubMed: 27556292]

Zhou Z, Li G, Lin C, He C. Conidiophore stalk-less1 encodes a putative zinc-finger protein involved in the early stage of conidiation and mycelial infection in Magnaporthe oryzae. Mol Plant Microbe Interact. 2009; 22:402–410. [PubMed: 19271955]

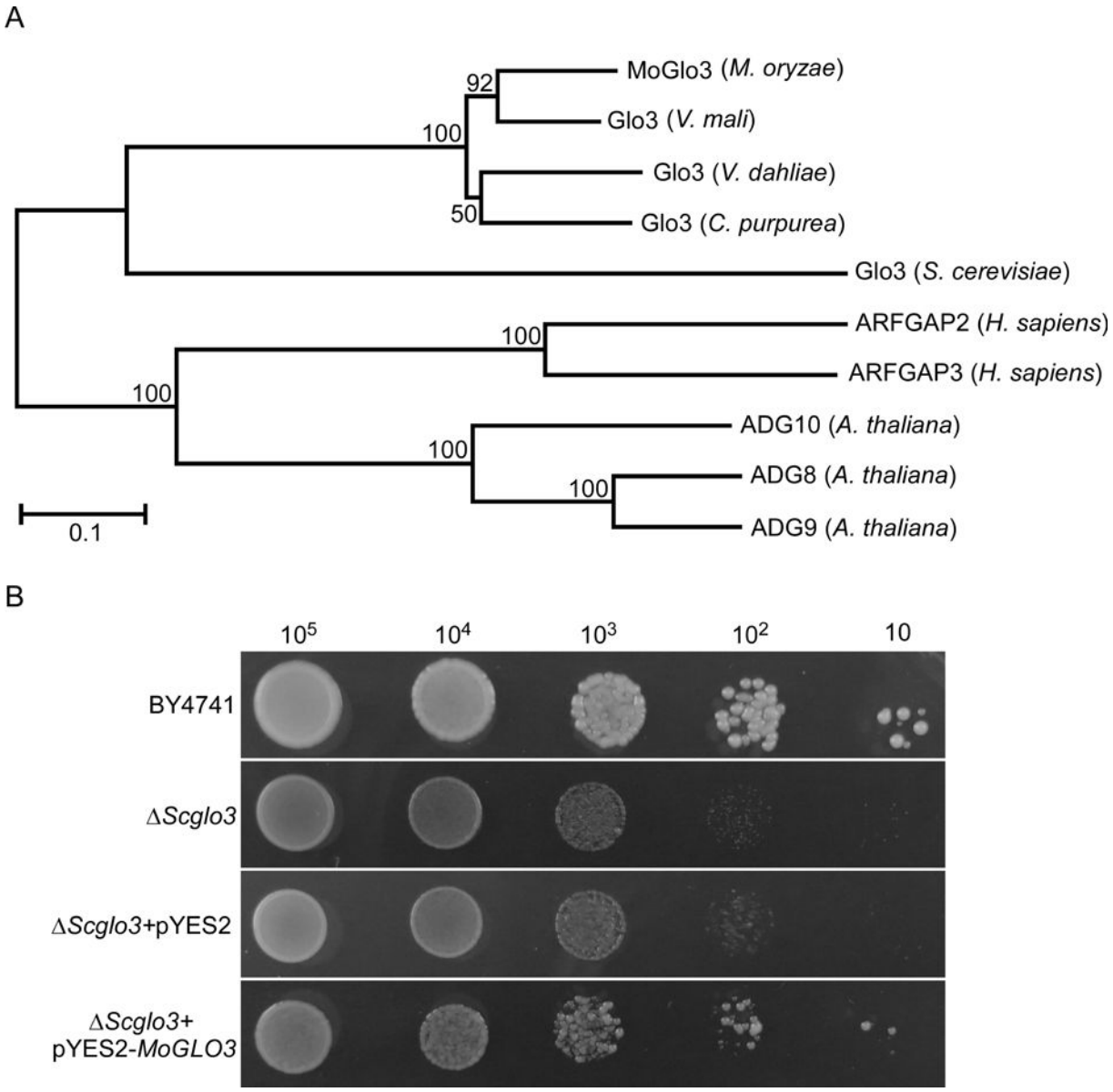

Figure 1. Phylogenetic analysis of MoGlo3 and yeast complementation assay

(A) The Glo3-type ArfGAPs from diverse organisms were aligned using the CLUSTAL_W and the neighbour-joining tree was constructed by MEGA 5.05 with 1000 bootstrap replicates. GenBank accession numbers and the corresponding species names are as follows: XP_ 003714430.1 (*Magnaporthe oryzae* MoGlo3); KUI69096.1 (*Valsa mali* var. *pyri* Glo3); XP_009650261.1 (*Verticillium dahliae VdLs.17* Glo3); CCE34127.1 (*Claviceps purpurea 20.1* Glo3); NP_011048.1 (*Saccharomyces cerevisiae* Glo3); NM_032389.4 (*Homo sapiens* ARFGAP2); NM_014570.4 (*Homo sapiens* ARFGAP3); NP_565801.1 (*Arabidopsis thaliana* ADG10); NP_567543.1 (*Arabidopsis thaliana* ADG8); NP_199487.1 (*Arabidopsis thaliana* AGD9).

(B) MoGlo3 partially rescued the growth of *S. cerevisiae* Δ*Scglo3* mutant. Serial dilutions of BY4741, Δ*Scglo3*, and Δ*Scglo3* transformed with pYES2 or pYES2-*MoGLO3* were grown on SD-Met-Leu-His-Ura (galactose) plates at 30°C for 4 days and then photographed.

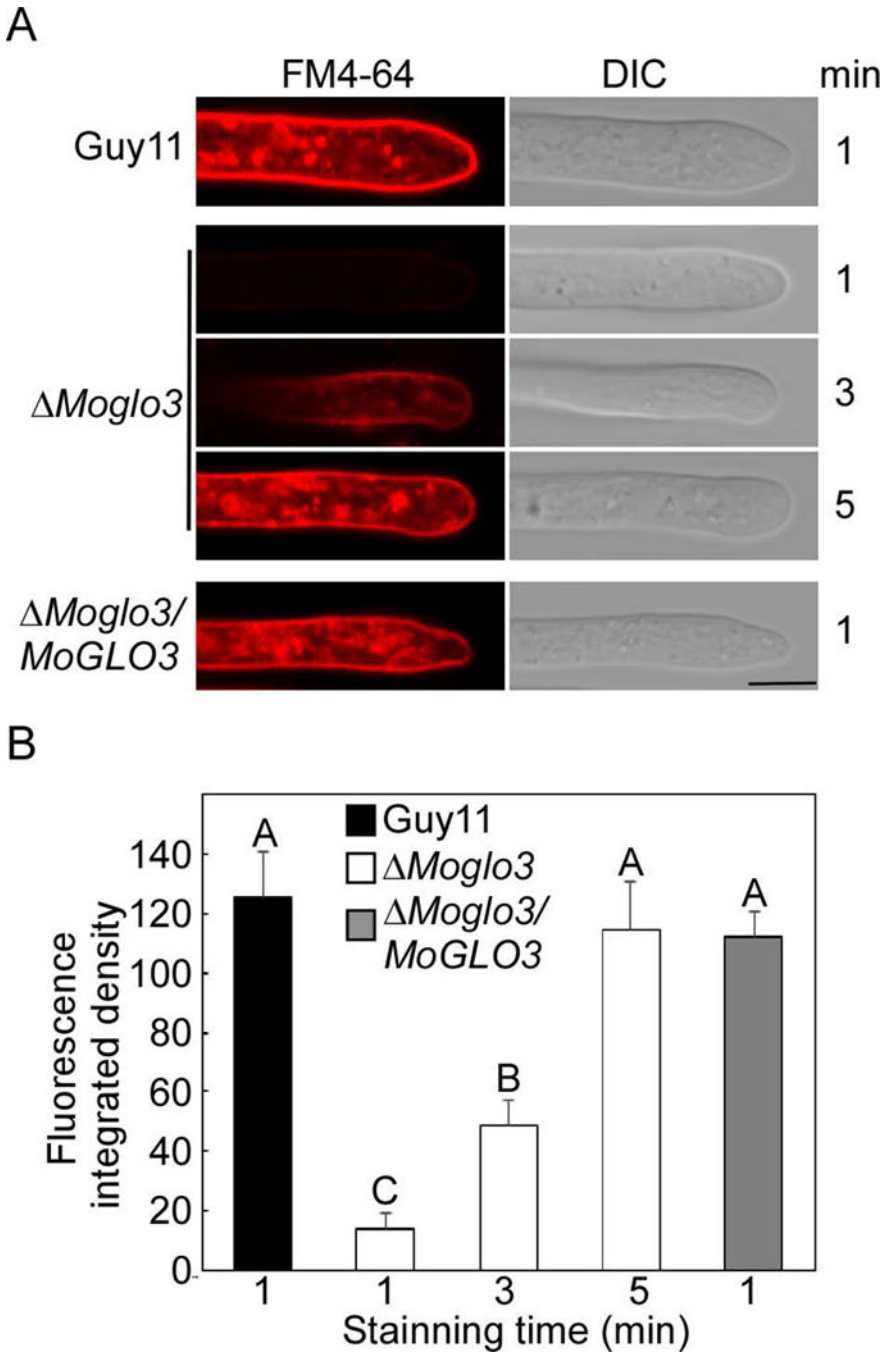

Figure 2. MoGlo3 plays a role in endocytosis

(A) Hypha of the wide-type, *ΔMoglo3* mutant and complemented strain were incubated in liquid CM for 24 h, and photos (Zeiss LSM710, 63x oil) were taken after stained with FM4-64 for several minutes. Bar = 5μm.

(B) The calculation of integrated fluorescent density with Image J. SD was calculated from three repeated experiments and different letters indicate statistically significant differences ($p < 0.01$).

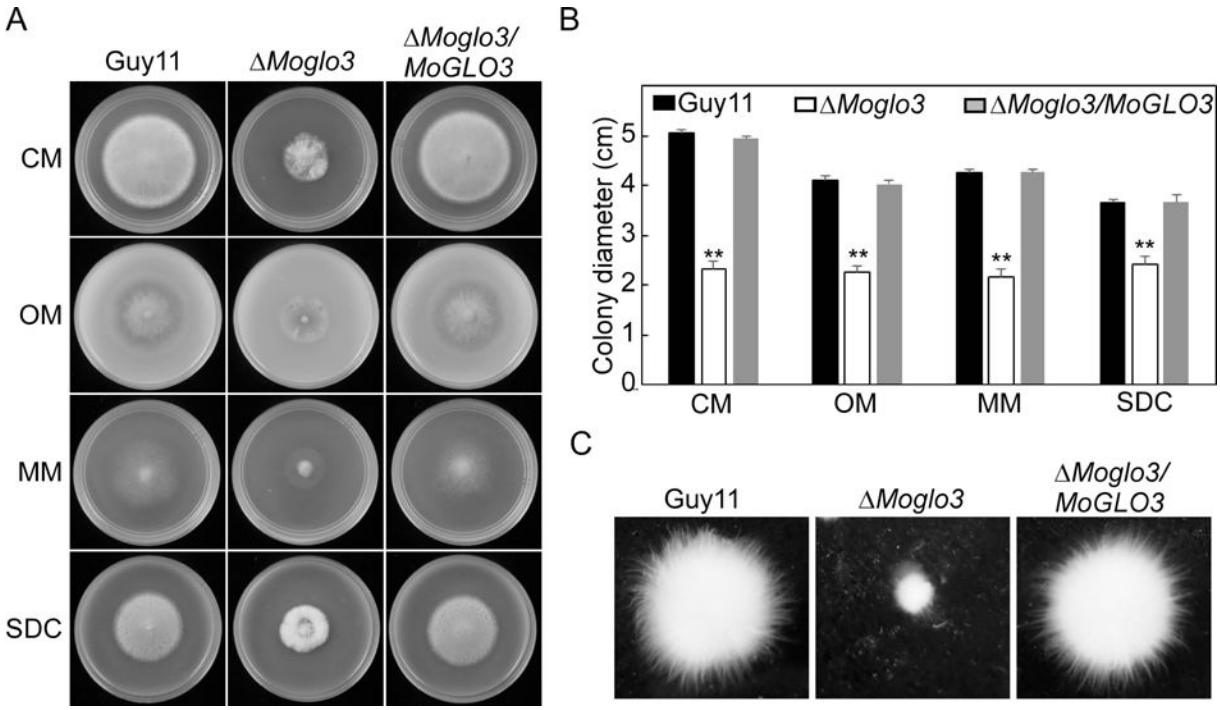

Figure 3. MoGlo3 plays a critical role in vegetative growth

(A) Growth of Guy11, the Δ*Moglo3* mutant and complemented strain in CM, OM, MM, SDC media, cultured in 28°C for 7 days and then photographed.

(B) Colony diameters were measured in each independent biological experiment and statistically analyzed by Duncan analysis. Asterisks represent significant differences ($p < 0.01$).

(C) Mycelial growth following inoculation in liquid CM for 48 h in 28°C was photographed.

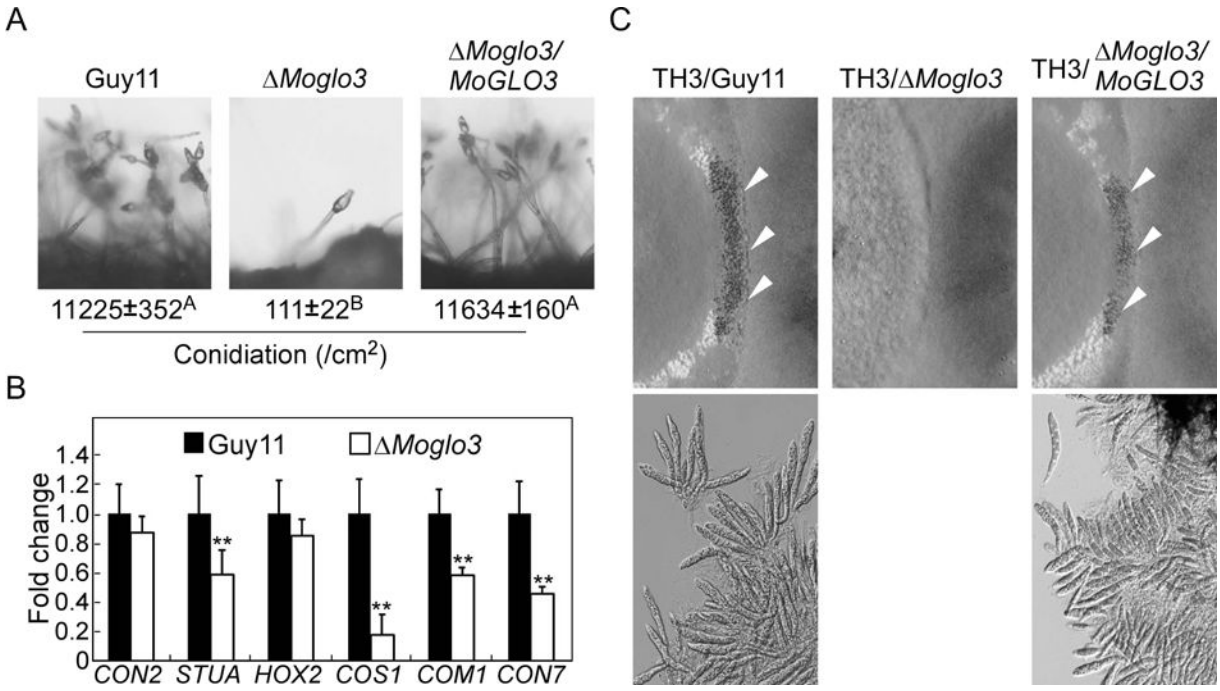

Figure 4. MoGlo3 is involved in asexual and sexual development

(A) Conidia formation was observed under a light microscope after induction of conidiation on glass slides for 16 h. The conidia produced by the tested strains grown on SDC medium for 10 days were collected, counted and analyzed by Duncan analysis ($p < 0.01$). Three independent experiments yielded similar results.

(B) Transcriptional expression patterns of conidiation-related genes in the wild-type Guy11 and Δ*Moglo3* mutant. Significant differences are indicated by asterisk ($p < 0.01$).

(C) Perithecia development and ascospore formation were photographed after four-week inoculation. Cross of TH3 (*MAT1-1*) with Guy11 (*MAT1-2*) represents the positive control. Arrows point to peritheria.

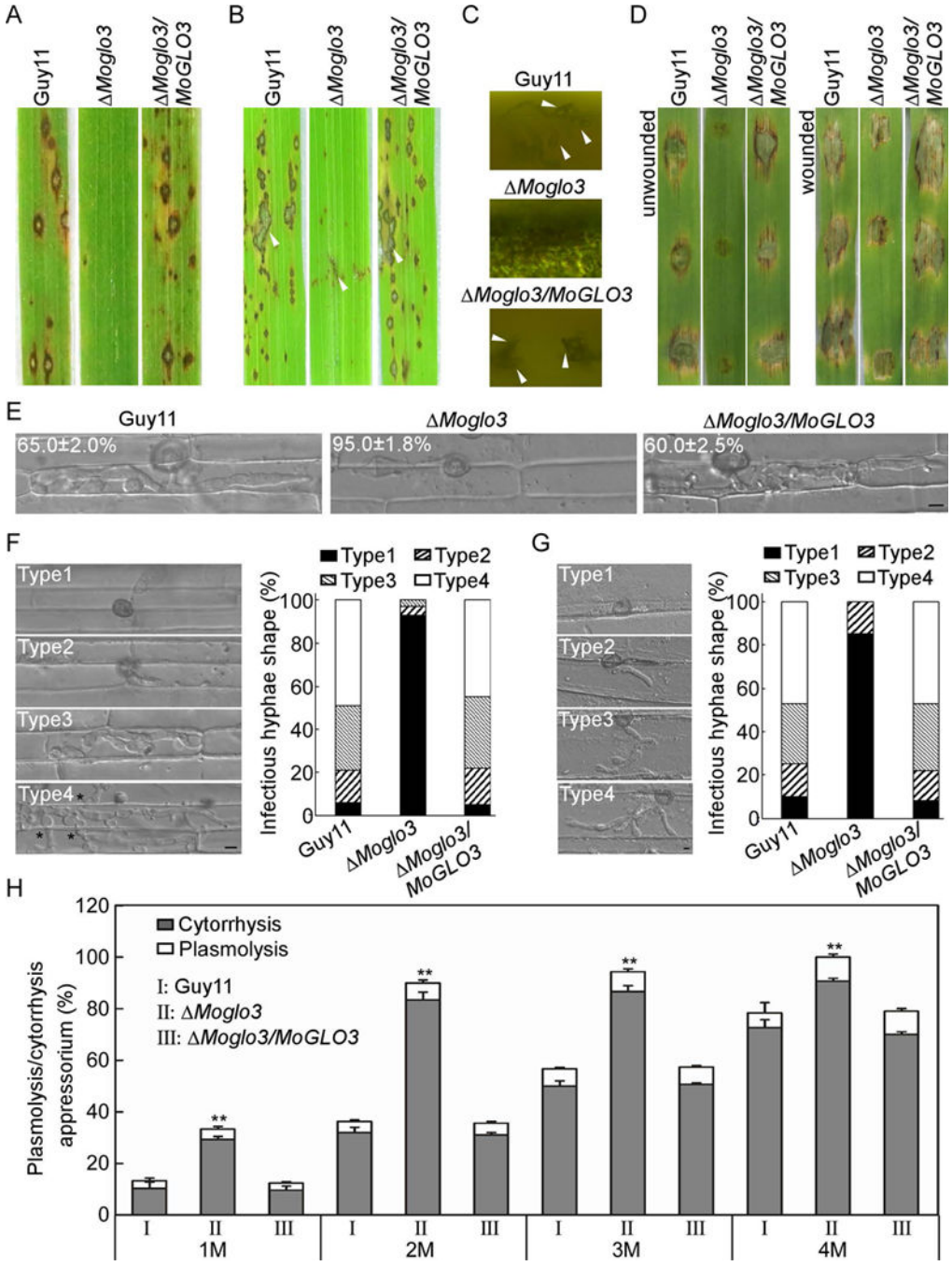

Figure 5. MoGlo3 is required for full virulence

(A) Pathogenicity was tested by spray assay with conidia (1×10^4 conidia/ml), and photographed at 7 days post-inoculation (dpi).

(B) Pathogenicity was tested by rice injection assay with conidia (5×10^4 conidia/ml), and photographed at 7 dpi. The arrowheads indicate injection sites.

(C) Microscope observation of the conidia development on lesions after illuminated for 24 h. Arrows indicate conidia.

(D) Pathogenicity was tested on unwounded and wounded barley leaves with conidia (5×10^4 conidia/ml), and photographed at 5 dpi.
(E) Comparative analysis of invasive hyphal growth of the strains in rice sheath cells at 24 hpi. Bar = 5 μm.
(F) Detailed observations and statistical analysis of invasive growth in the cells of rice at 48 hpi. One hundred appressorium penetration sites were counted for each strain and the invasive hypha were rated from type 1 to 4 (Type1, no penetration; Type2, with a penetrating peg; Type3, extend but limit in one cell; Type4, extend to neighboring cells). Asterisks indicate hyphae extended to neighboring cells. The experiments were repeated three times. Bar = 5 μm.
(G) Detailed observations and statistical analysis of invasive growth in cells of barley leaves. One hundred appressorium penetration sites were counted for each strain and the invasive hypha were rated from type 1 to 4 (Type1, no penetration; Type2, with a penetrating peg; Type3, with two or three invasive hypha; Type4, with more than three invasive hypha). The experiments were repeated three times. Bar = 5 μm.
(H) Statistical analysis of appressoria exhibited plasmolysis and cytorrhysis in different glycerol concentration. Error bars represent the standard deviations and asterisks represent significant differences ($p < 0.01$).

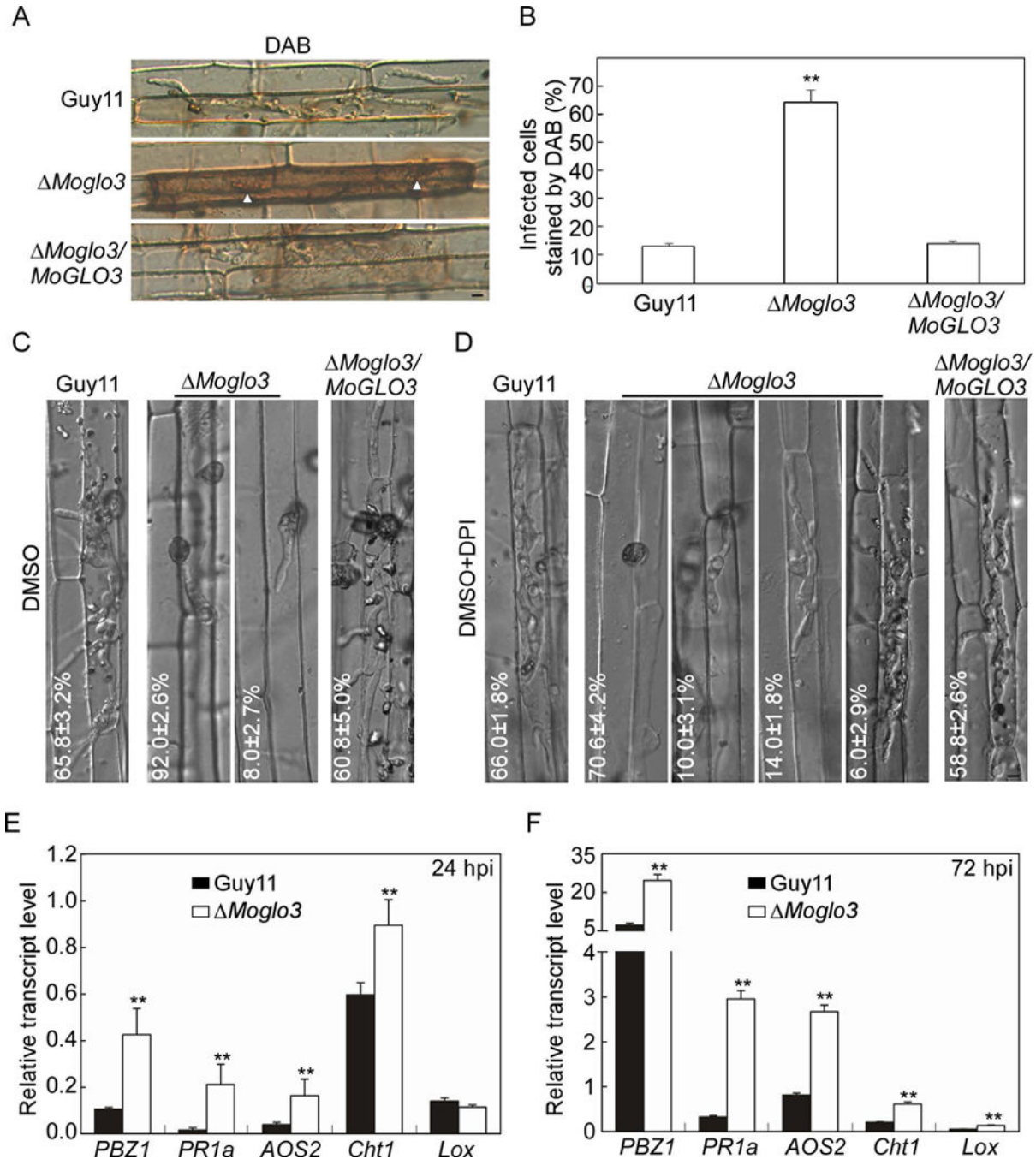

Figure 6. MoGlo3 is involved in scavenging of ROS

(A) The excised rice sheaths were injected with related conidial suspensions. DAB was used to stain the sheaths for 8 h after 30 hpi. Bar = 5 μm.

(B) Statistical analysis for the percentages of cells with infectious hypha dyed by DAB. Means were calculated from three independent replicates. Asterisks represent significant differences ($p < 0.01$; n = 100).

(C, D) Statistical analysis of different infectious hypha types in rice cells inoculated with conidial suspensions treated with or without 0.5 μM DPI dissolved in DMSO. The treatment

of DMSO was a negative control. SD was calculated from three repeated experiments. Bar = 5 μm.

(E, F) Expression analysis of defense-related genes by qRT-PCR at 24 hpi and 72 hpi. The average threshold cycle of triplicate reactions was normalized to elongation factor 1a (*EF1a*, Os03g08020) in *O. sativa*, asterisks represent significant differences. Three independent biological experiments were performed and yielded similar results.

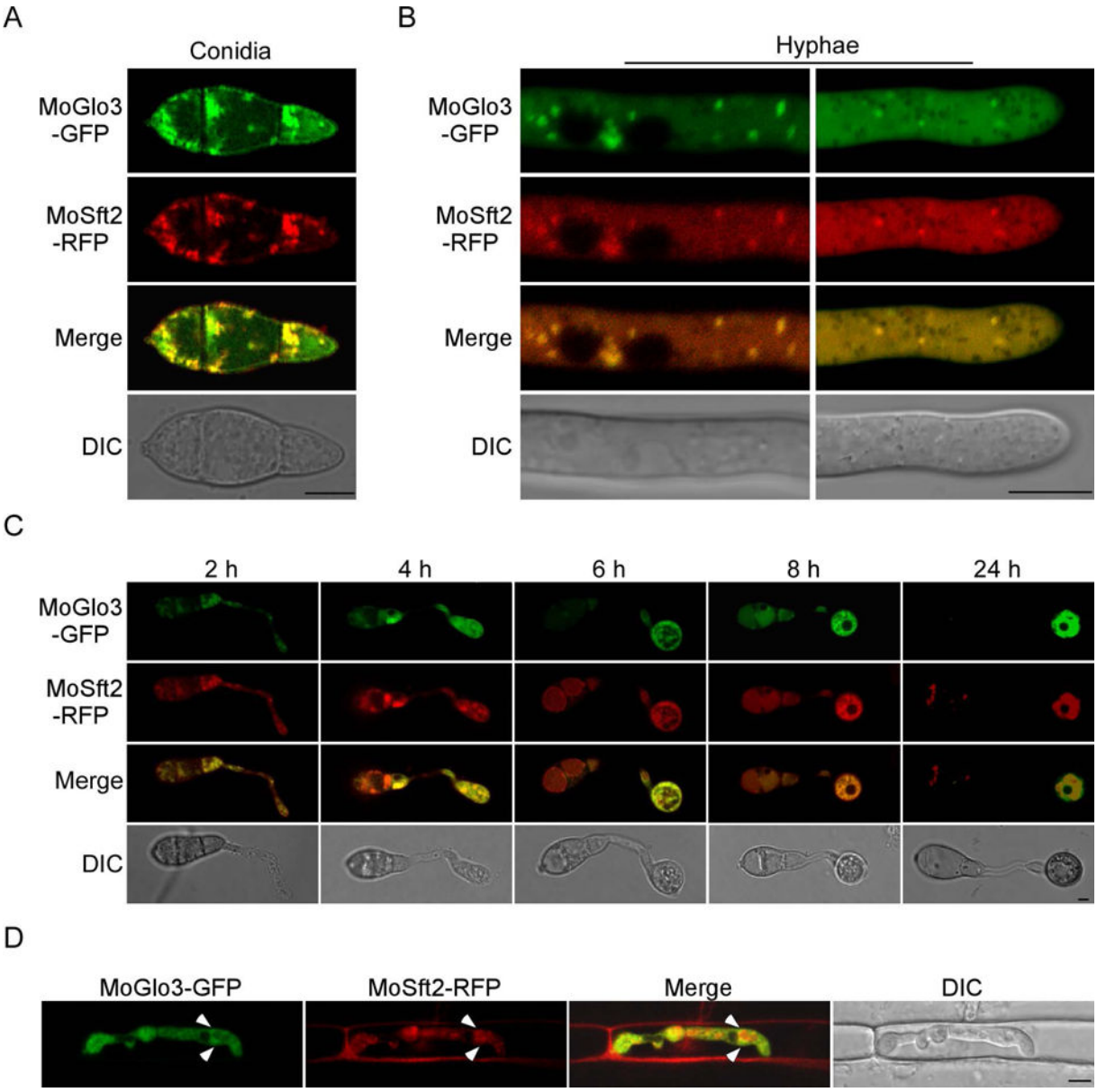

Figure 7. MoGlo3 localizes to Golgi apparatus

(A, C) The localization pattern of MoGlo3 in the conidia and conidia inoculated on coverslips for 2, 4, 6, 8 and 24 h. Shown are confocal fluorescent images (Leica TCS SP8, 100x oil), indicating co-localization of MoGlo3 with MoSft2 which was expressed as a Golgi marker. Bar = 5 μm.

(B, D) Localization pattern of MoGlo3 in the hypha and invasive hypha. Shown are confocal fluorescent images (Zeiss LSM710, 63x oil), indicating co-localization of MoGlo3 with MoSft2. Arrows indicate Golgi. Bar = 5 μm.

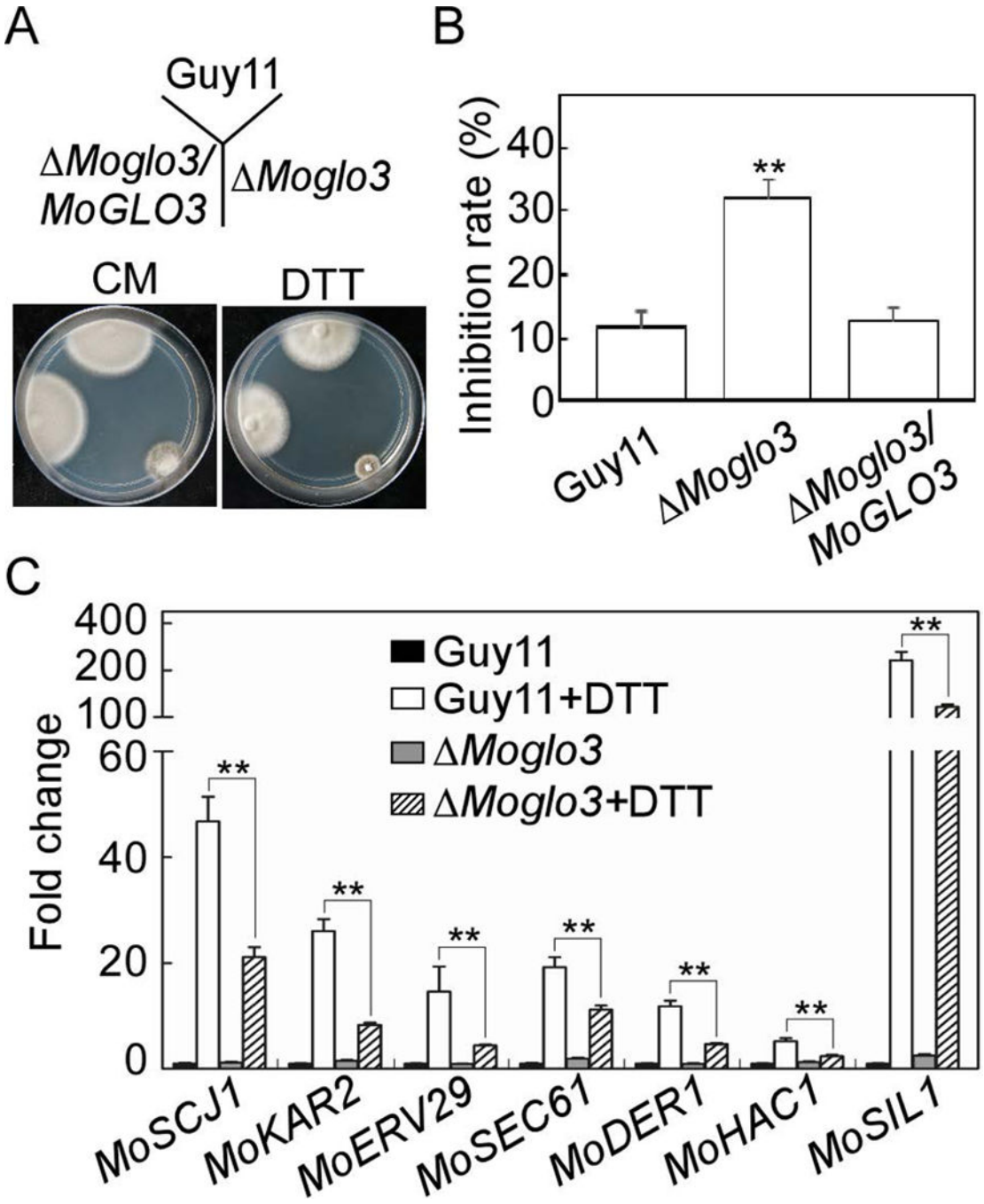

Figure 8. MoGlo3 participates in the response to ER stress

(A) Wild-type Guy11, *ΔMoglo3* mutant and complemented strain were incubated in CM media or CM media supplemented with 2.5 mM DTT at 28°C for 7 days.

(B) Statistical analysis of inhibition rates of the strains to DTT stress. Three independent biological experiments were performed with three replicates each time, and similar results yielded in each biological experiment. Error bars represent SD of three replicates and asterisks represent significant difference between Guy11 and Δ*Moglo3* mutant ($p < 0.01$).

(C) Loss of MoGlo3 affects the regulation of UPR pathway. Expression analysis of six putative UPR-related genes (*MoSCJ1*, *MoKAR2*, *MoERV29*, *MoSEC61*, *MoDER1*, and *MoSIL1*) and *MoHAC1* in Guy11 and Δ*Moglo3* mutant with or without DTT treatment by qRT-PCR. Asterisks represent significant differences ($p < 0.01$). Three independent biological experiments were performed and yielded similar results.

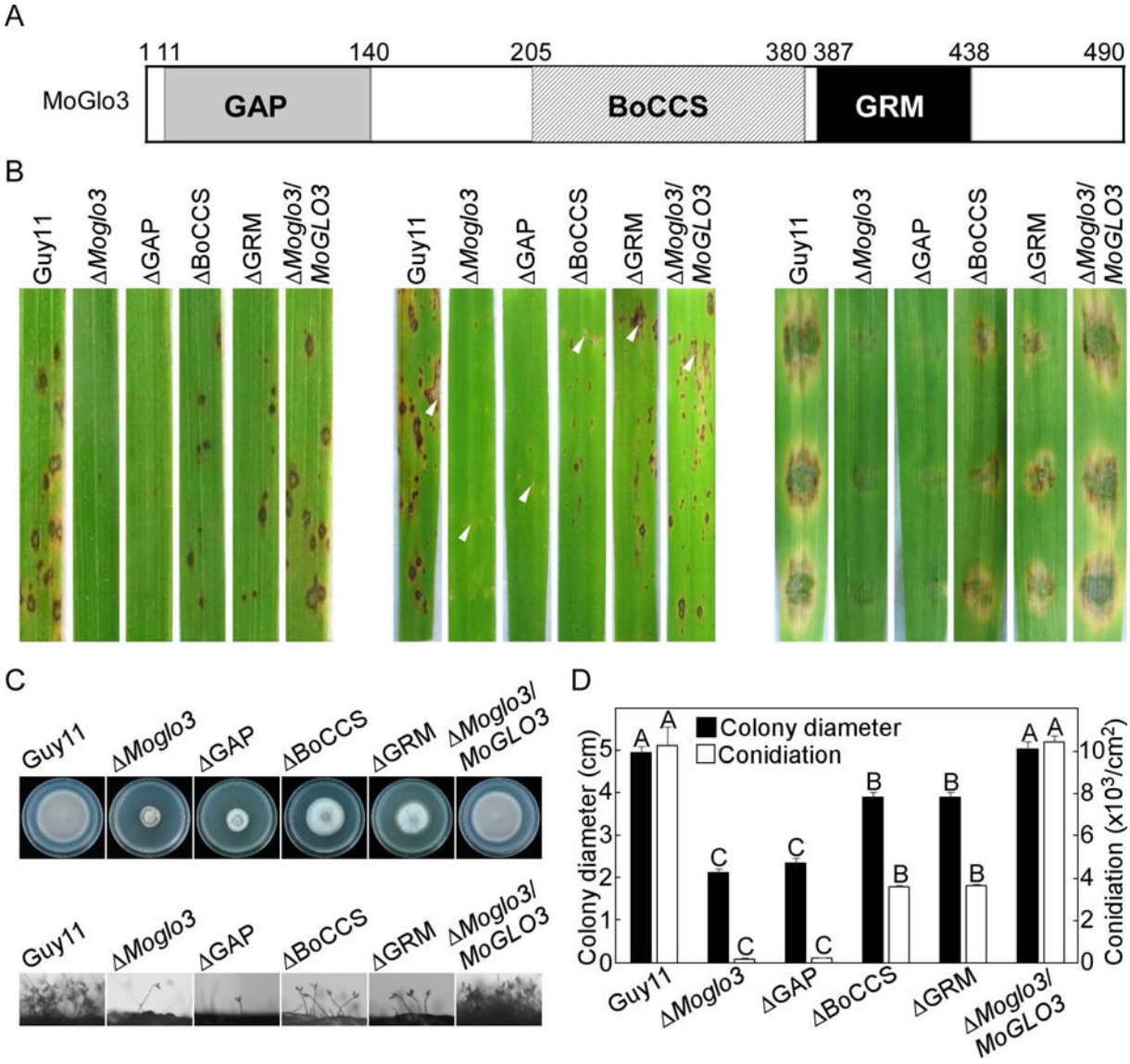

Figure 9. GAP, BoCCS and GRM are essential for the function of MoGlo3

(A) Structure and domain prediction of MoGlo3. The positions of the domains within the proteins were indicated by amino acid numbers.

(B) GAP-deleted domain of MoGlo3 resulted in similar pathogenicity defects to Δ*Moglo3* mutant by sprayed (left panel) and injected (middle panel) rice assay and detached barley (right panel) assay. BoCCS-deleted and GRM-deleted strain incompletely recovered the pathogenicity defects of the mutant.

(C) Images of conidial development and growth test of the indicated strains.

(D) Statistical analysis of the colony diameter and conidiation of different strains. SD was calculated from three repeated experiments and different letters indicate statistically significant differences ($p < 0.01$).

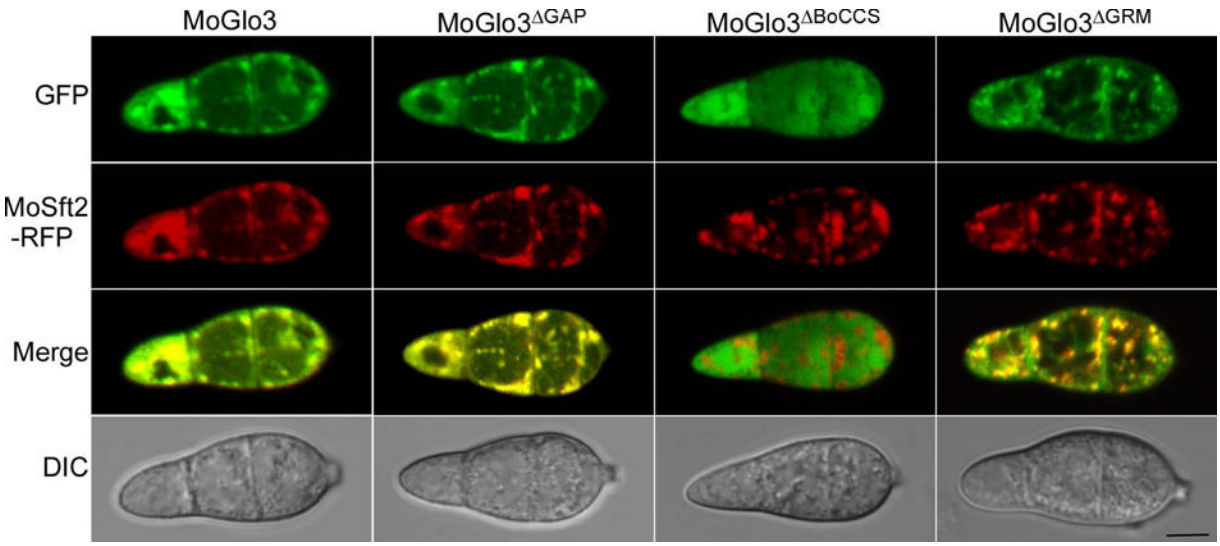

Figure 10. Subcellular localization of different truncated MoGlo3

Localization pattern of different truncated MoGlo3 in the conidia. Shown are confocal fluorescent images (Zeiss LSM710, 63x oil), indicating the deleted GAP or GRM of the protein still co-localized with MoSft2, However, deleted BoCCS domain of truncated MoGlo3-GFP distributed throughout the cytoplasm. Observations were replicated in at least three experiments. Bar = 5 μm.